

Article

Temperature Estimation of Stator Winding in Permanent Magnet Synchronous Motors Using d -Axis Current Injection

Bum-Su Jun ¹, Joon Sung Park ² , Jun-Hyuk Choi ², Ki-Doek Lee ² and Chung-Yuen Won ^{1,*}

¹ Department of Electrical and Computer Engineering, Sungkyunkwan University, Suwon 16419, Korea; cvcy@skku.edu

² Intelligent Mechatronics Research Center, Korea Electronics Technology Institute (KETI), Bucheon 14502, Korea; parkjs@keti.re.kr (J.S.P.); cjh@keti.re.kr (J.-H.C.); kdlee@keti.re.kr (K.-D.L.)

* Correspondence: woncy@skku.edu; Tel.: +82-31-290-4963

Received: 9 July 2018; Accepted: 30 July 2018; Published: 6 August 2018



Abstract: This paper presents a stator winding temperature detection method for permanent magnet synchronous motors (PMSMs) using a motor parameter estimation method. PMSM performance is highly dependent on the motor parameters. However, the motor parameters vary with temperature. It is difficult to measure motor parameters using a voltage equation without additional sensors. Herein, a stator winding temperature estimation method based on a d -axis current injection method is proposed. The proposed estimation method can be used to obtain stator temperatures and to achieve reliable operation. The validity of the proposed method is verified through simulations and experimental results.

Keywords: permanent magnet synchronous motor (PMSM); motor parameter estimation; stator winding temperature estimation; d -axis current injection; stator winding resistance

1. Introduction

Permanent magnet synchronous motors (PMSMs) are widely employed in industrial drives, electric vehicles, renewable energy systems, etc., owing to their high torque density, high power density, and high efficiency [1]. The motors, primarily applied in drones and fans, are of the outer rotor type, in which the rotor is located outside and the stator is located inside. These motor types are surface-mounted permanent magnet synchronous motors (SPMSMs) with the same d -axis inductance and q -axis inductance. The torque is generated only by the q -axis current. In outer-rotor-type motors, the stator is located inside and temperature rises may occur and, as such, turn faults may occur as well. The life of the motor can be reduced by approximately 50% for every 10 °C increase in the stator winding temperature design limit [2,3]. The motor parameters are dependent on current and temperature. Due to high temperatures, or high currents, turn faults [4–6] in the stator may occur. Current can be easily measured using the current sensors of the inverter. However, it is difficult to obtain the internal temperature of the motor, especially that of the stator winding.

Among all temperature monitoring methods, the most accurate is to insulate temperature sensors [3]. However, the insulation of the temperature sensor is not cost-effective and temperature sensor reliability problems may occur. Motor internal temperature estimation methods can be classified into thermal model methods [7–10], and motor parameter estimation methods [11–15]. The lumped-parameter thermal network [7] is the most well-known thermal model method. The thermal model system is an eighth-order dynamic model, with many thermal capacitances and resistances, either directly acquired from various experimental tests, or derived from the dimensions

and material thermal properties of the motor. However, with some assumptions in place, a few simplified thermal models have been proposed [8–10]. The computations are less complicated, but the thermal models are still significant with many model parameters able to be identified from simulations and experimental tests. The thermal model is highly dependent on the cooling system and the geometry of the motor, and specific analysis for each motor design and application is required. These results lead to limited applications and require long development times. In the parameter estimation method, stator resistance is used as the indicator of the stator winding temperature. This approach has significant advantages over the thermal model method. The accuracy of the stator temperature estimation is not affected by the motor specifications, cooling method, or operating conditions [11,12], and the stator resistance can be estimated from the electrical equivalent model of the motor [13]. However, the stator resistance is significantly small and the performance of the temperature estimation is too sensitive to motor inductance variations [2]. To improve the accuracy of the stator resistance estimation, an inductance map and back electromotive force (BEMF) map are required. The inductance map and BEMF map are identified from the simulations and experimental results. These factors lead to long development times being required.

This paper presents a stator winding temperature estimation method for motor systems without additional temperature sensors. To obtain the stator winding temperature, the motor parameters are estimated. The estimated parameters enable the stator winding temperature to be obtained because the parameters vary with temperature. For the motor parameter estimation, the d -axis current injection method is proposed. This paper is organized as follows: the principles and analysis of the SPMSM operation are presented in Section 2; the proposed estimation method is analyzed in Section 3; simulation and experimental results are described in Sections 4 and 5 to evaluate the performance of the temperature estimation; and finally, conclusions are presented in Section 6.

2. Operations of PMSMs

The fundamental model of PMSMs in the synchronous reference frame is given by [14–16]:

$$\begin{cases} v_d^e = R_s i_d^e - \omega_r L_q i_q^e + p L_d i_d^e \\ v_q^e = R_s i_q^e + \omega_r L_d i_d^e + p L_q i_q^e + \omega_r \psi_m \\ T_e = \frac{3}{2} \frac{P}{2} \left[(L_d - L_q) i_d^e i_q^e + \psi_m i_q^e \right], \end{cases} \quad (1)$$

where $v_{d,q}^e$ and $i_{d,q}^e$ are the d -, q -axis stator voltage and current vectors in the synchronous reference frame, respectively. R_s and $L_{d,q}$ are the stator resistance and d -, q -axis inductance. The equivalent circuit of PMSMs is shown in Figure 1. The motor speed and the rotor flux are denoted by ω_r and ψ_m , respectively. p and P are the differential operator and the motor poles, respectively.

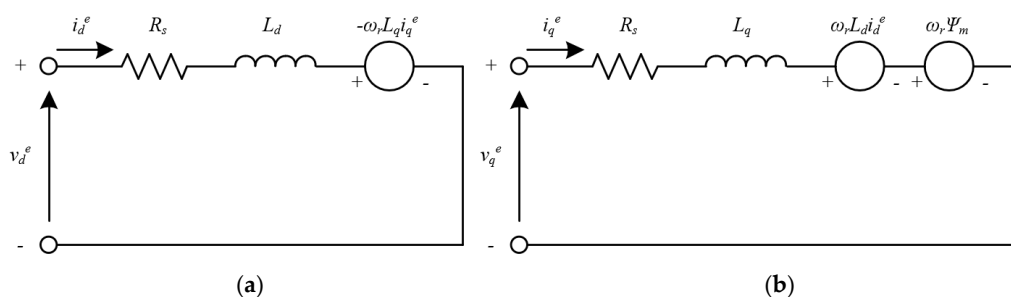


Figure 1. Equivalent circuit of permanent magnet synchronous motors (PMSMs): (a) d -axis; (b) q -axis.

Assuming the steady-state condition, voltage Equation (1) can be approximated as Equation (2). It is noteworthy that $\omega_r L_{d,q} i_{d,q}^e$ are the coupling terms, and that $\omega_r \psi_m$ is the BEMF voltage. Based on Equation (2), the voltage and current vectors are described in Figure 2 [16].

$$\begin{cases} v_d^e = R_s i_d^e - \omega_r L_q i_q^e \\ v_q^e = R_s i_q^e + \omega_r L_d i_d^e + \omega_r \psi_m \end{cases} \quad (2)$$

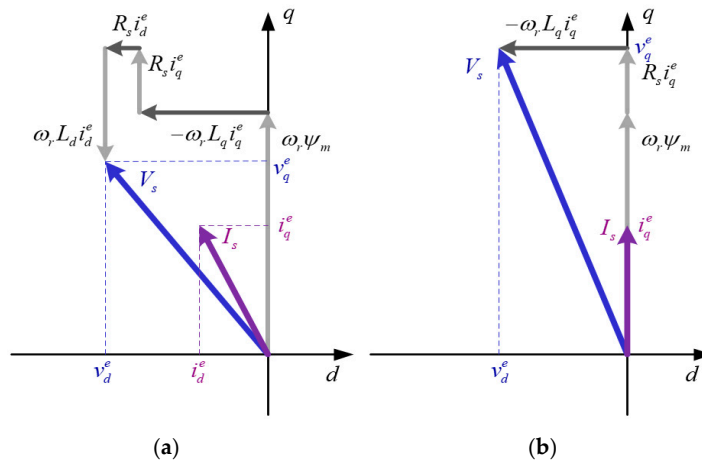


Figure 2. Voltage and current vectors when: (a) $i_d^e < 0, i_q^e > 0$; (b) $i_d^e = 0, i_q^e > 0$.

As shown in Equation (1), the electrical torque is composed of the magnetic torque and the reluctance torque. The magnetic torque is from the Lorentz force, and the reluctance torque is oriented from the L_d, L_q asymmetry [17,18]. Because the inductances L_d, L_q are equal for the SPMSMs, the reluctance torque becomes zero, and the torque equation can be rewritten as

$$T_e = \frac{3}{2} \frac{P}{2} \psi_m i_q^e. \quad (3)$$

The electrical torque for the SPMSMs can be controlled using the q -axis current. The constant torque curves of the SPMSMs are shown in Figure 3. The torque of the SPMSMs is generated by the q -axis current and the d -axis current does not contribute to torque generation.

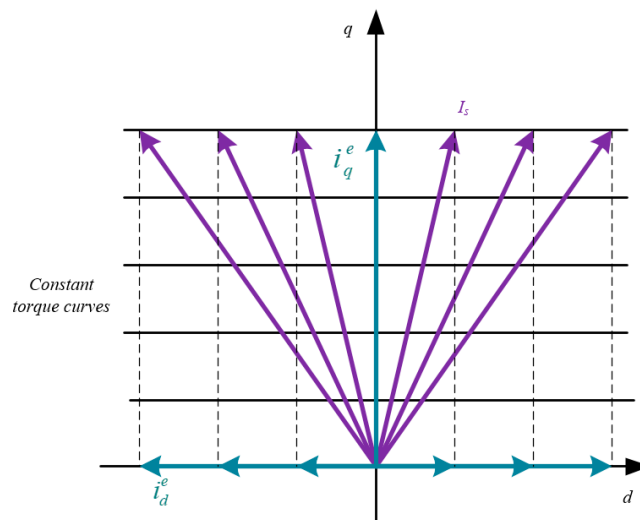


Figure 3. Constant torque curves for surface-mounted permanent magnet synchronous motors (SPMSMs).

Figure 4 shows the conventional control configuration of SPMSMs for speed control. Because the torque of SPMSMs is generated by the q -axis current, the d -axis current command is set to zero, and the q -axis current is used to construct the speed controller. Information about position and speed is measured by the position sensor. The q -axis current command is determined by the speed controller, and the d -, q -axis current controllers generate the d -, q -axis voltage references. The pulse width modulation (PWM) duties are determined using the space vector PWM method, based on the voltage reference in the synchronous reference frame. Finally, PWM duties are applied to the power switch using the gate drive of the inverter.

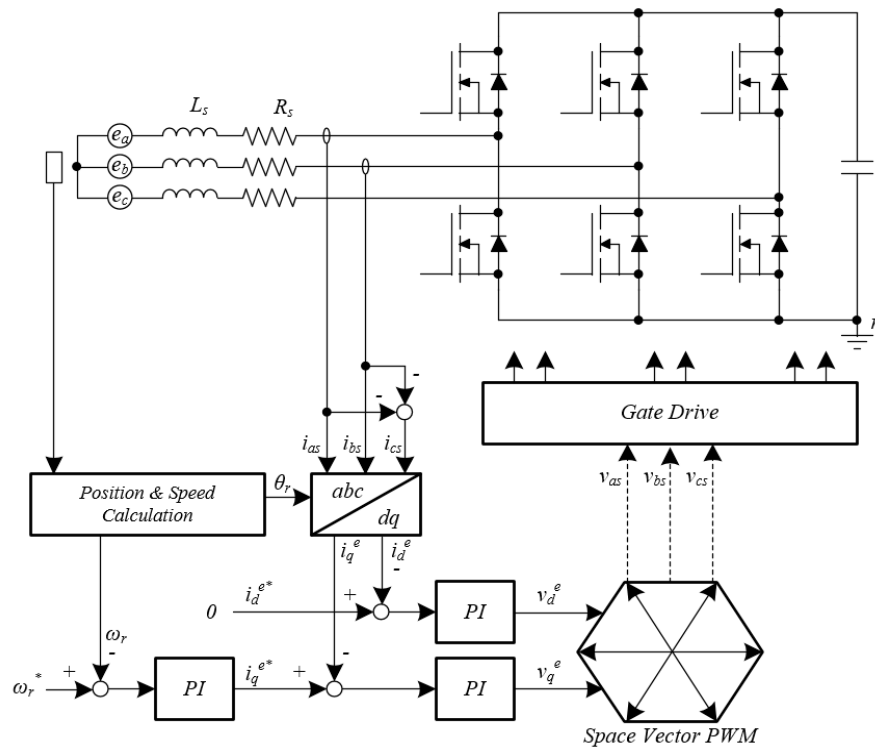


Figure 4. Conventional control configuration for SPMSMs.

3. Stator Winding Temperature Estimation Using d -Axis Current Injection

A temperature increase can cause several adverse effects [18,19]. For example, a temperature rise in the stator winding causes stator resistance variation and can degrade the stator winding insulation. The stator winding temperature can be detected through estimation of the stator resistance.

Under the steady-state condition, the voltage equation of PMSMs can be expressed as a variable depending on the temperature and current as

$$\begin{cases} v_d^e = R_s i_d^e - \omega_r L_q i_q^e \\ v_q^e = R_s i_q^e + \omega_r L_d i_d^e + \omega_r \psi_m \end{cases} \quad (4)$$

In Equation (4), R_s and ψ_m are functions of the stator and magnet temperatures, respectively. $L_{d,q}$ are the functions of the magnet temperature and the stator current. Equation (4) can be rewritten as Equation (5), because the d -axis current becomes zero for the torque maximization of SPMSMs:

$$\begin{cases} v_d^e = -\omega_r L_q i_q^e \\ v_q^e = R_s i_q^e + \omega_r \psi_m \end{cases} \quad (5)$$

From Equation (5), the q -axis inductance can be expressed as Equation (6).

$$L_q = -\frac{v_d^e}{\omega_r i_q^e} \tag{6}$$

$$R_s = \frac{v_q^e - \omega_r \psi_m}{i_q^e} \tag{7}$$

The stator temperature can be estimated through the calculation of the stator resistance, as in Equation (7). However, as the rotor flux can vary with the rotor temperature, the stator winding temperature estimation may exhibit low accuracy. This may cause a large error in the temperature estimation of the stator winding. Therefore, an additional equation is required to obtain the stator winding temperature.

As mentioned in the previous section, the constant torque for the SPMSMs is maintained even if the d -axis current is applied while the constant q -axis current is generated. Under the constant torque operation, the motor speed is maintained, and Equation (4) can be expressed. Figure 5 shows voltage and current vectors for temperature estimation. The d -axis current injection can be performed while the q -axis current is constant. When the d -axis current i is injected, the voltages and currents can be expressed as $v_d^e(i)$, $v_q^e(i)$, and $i_d^e(i)$, $i_q^e(i)$, respectively. When $i_d^e = 0$, the voltage and the current can be expressed as $v_d^e(0)$, $v_q^e(0)$, and $i_d^e(0)$, $i_q^e(0)$, respectively. The voltage equation for generating the same torque can be summarized as Equations (8) and (9).

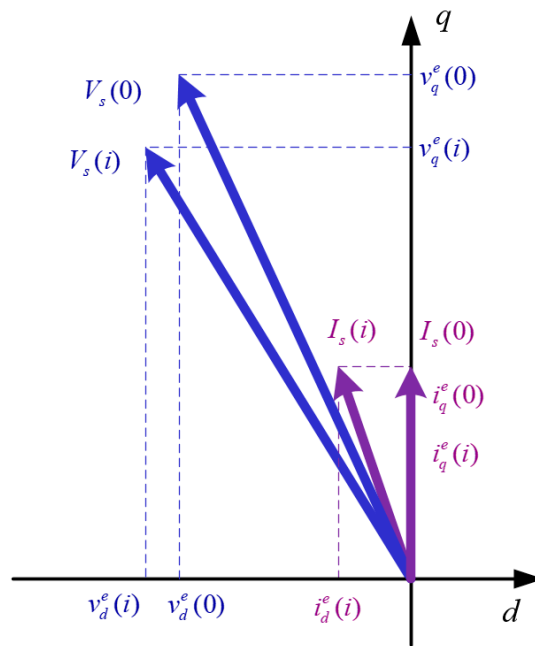


Figure 5. Voltage and current vectors for temperature estimation.

$$\begin{cases} v_d^e(i) = R_s i_d^e(i) - \omega_r L_q i_q^e(i) \\ v_q^e(i) = R_s i_q^e(i) + \omega_r L_d i_d^e(i) + \omega_r \psi_m \end{cases} \tag{8}$$

$$\begin{cases} v_d^e(0) = -\omega_r L_q i_q^e(0) \\ v_q^e(0) = R_s i_q^e(0) + \omega_r \psi_m \end{cases} \tag{9}$$

Because the currents, motor speed, and voltage can be measured or calculated by the current sensor, position sensor, and current controller output, the q -axis inductance can be calculated as Equation (10)

from Equation (9). We can assume Equation (10) because the difference between the d -axis inductance and the q -axis inductance is sufficiently small.

$$L_d = L_q = -\frac{v_d^e(0)}{\omega_r i_q^e(0)} \quad (10)$$

Equation (10) can be substituted into Equation (8) and arranged as Equation (11). The phase resistance R_s can be derived by using Equations (11) and (12).

$$v_d^e(i) = R_s i_d^e(i) + v_d^e(0) \frac{i_q^e(i)}{i_q^e(0)} \quad (11)$$

$$R_s = \frac{v_d^e(i)}{i_d^e(i)} - \frac{v_d^e(0)}{i_d^e(i)} \frac{i_q^e(i)}{i_q^e(0)} \quad (12)$$

Based on finite element analysis (FEA), the SPMSMs can be modeled and analyzed. The R_s map according to the stator winding temperature can be obtained from the FEA results. The stator winding temperature can be estimated by comparing the calculated R_s with the temperature map. Analysis is not required regarding the inductance and the rotor flux variation according to the current vectors and the magnet temperature using FEA, because the d -, q -axis inductances can be calculated as shown in Equation (10) and the rotor flux is not required to calculate the stator resistance.

Figure 6 shows the control block-diagram of the proposed stator winding temperature estimation method using the motor parameter estimation for the SPMSMs. As described above, two equations, depending on whether the d -axis current is injected or not, are required for estimating the stator temperature. To detect the stator temperature, the output d -, q -axis currents, the applied d -, q -axis voltages, and the motor speed are stored when $i_d^e = 0$. Subsequently, the d -axis current is applied in the same q -axis current to measure the output d -, q -axis currents, the applied d -, q -axis voltages, and the motor speed. The d -axis current should be applied considering the current limit. After the detection of variables for the temperature estimation, the d -axis current is again applied at zero. The stator resistance is estimated using Equation (12). The stator winding temperature is estimated using the look-up table obtained from FEA. An averaging filter can be used in consideration of inverter noise during data acquisition. The estimation time is determined by the response performance of the current controller and filtering. The stator winding temperature estimation procedure does not need to be continuously operated, and the stator winding temperature can be estimated by applying the d -axis current only when the stator winding temperature is required. A rectangular d -axis current, can be used to estimate the stator winding temperature.

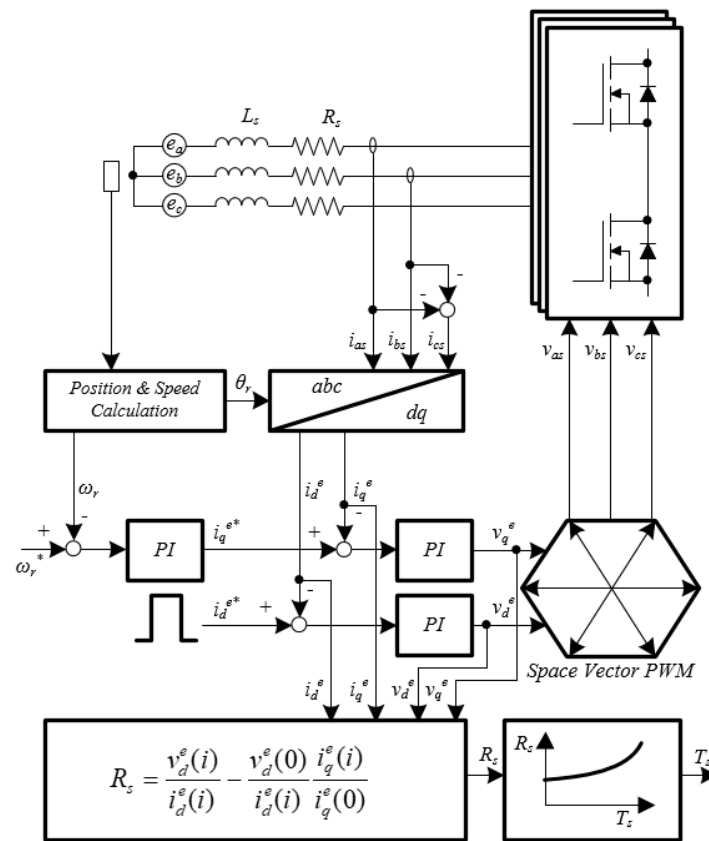


Figure 6. Proposed control block-diagram for stator winding temperature estimation.

4. Simulation Results

Finite element modeling (FEM) was used for the verification of motor parameter variation. The motor design used for the motor parameter variation simulation with temperature is shown in Figure 7, and the motor parameters at 20 °C are shown in Table 1.

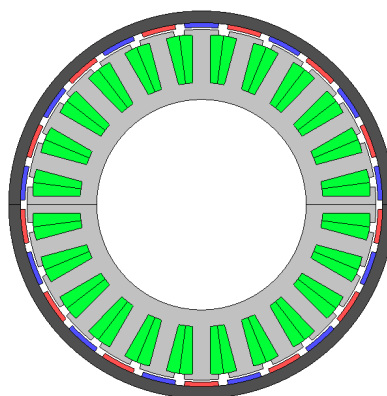


Figure 7. SPMSM design.

Table 1. Motor parameters at 20 °C.

Poles	Turns	Coil Diameter	I_{rated}	V_{dc}	Slots	Connection	R_s	L_d/L_q	ψ_m
26	19	0.6mm	11 A	52 V	24	Y	0.0777 Ω	0.08 mH	0.00335 Wb

Figure 8 shows the stator resistance as a function of temperature. As the temperature increases, the stator resistance increases. The stator resistance can be calculated from Equation (12). The stator winding temperature can be estimated using the resistance table as shown in Figure 8.

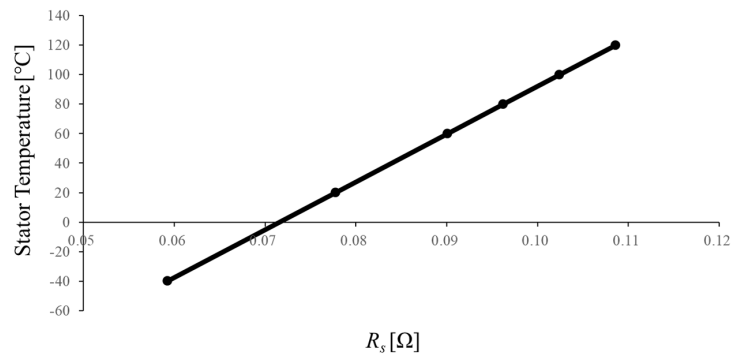


Figure 8. Motor parameter map according to stator winding temperature.

Figure 9 shows the d - and q -axis inductance maps according to i_d and i_q at 20 °C. Unlike stator resistance, motor inductance varies with rotor temperature and current. Therefore, the inductance in the simulation should vary according to the temperature and the current. The inductance map was derived from the FEM analysis and applied to motor modeling.

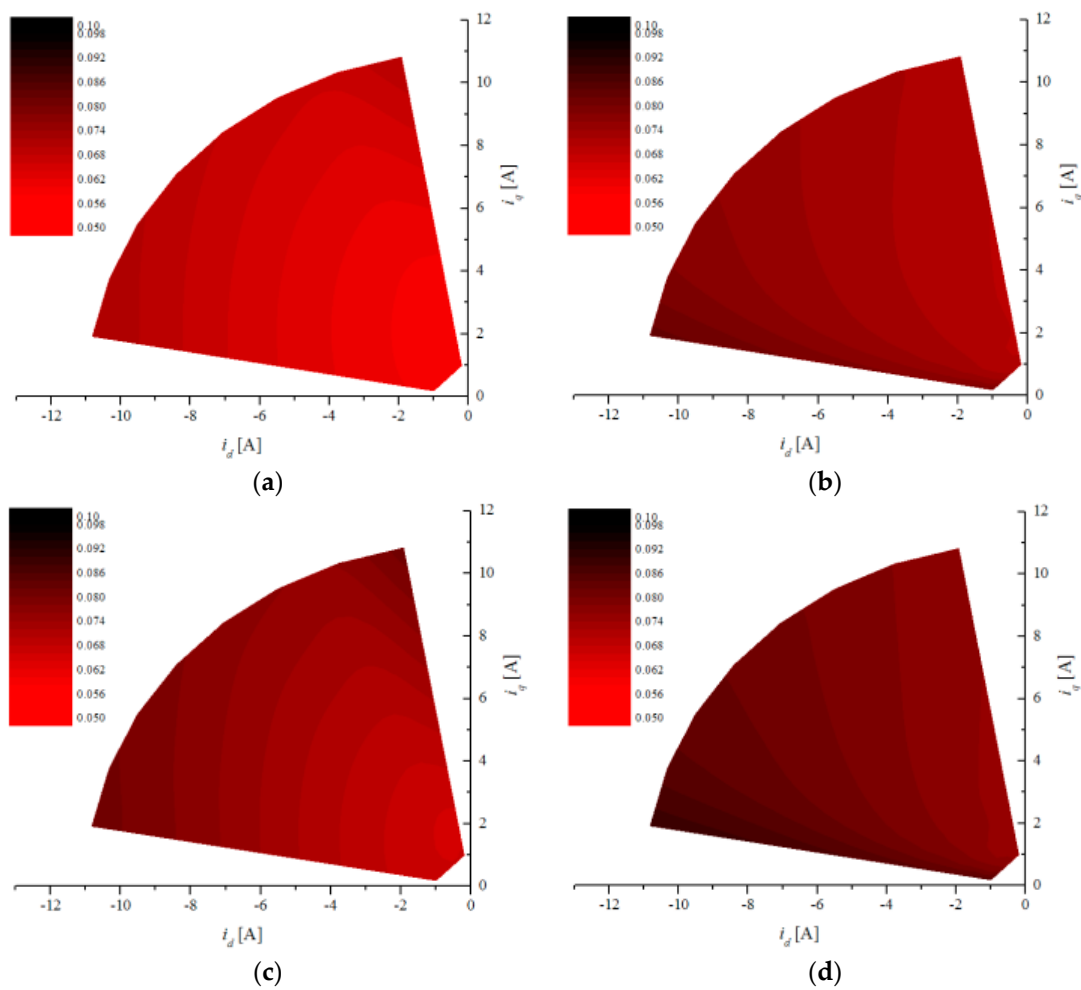


Figure 9. Cont.

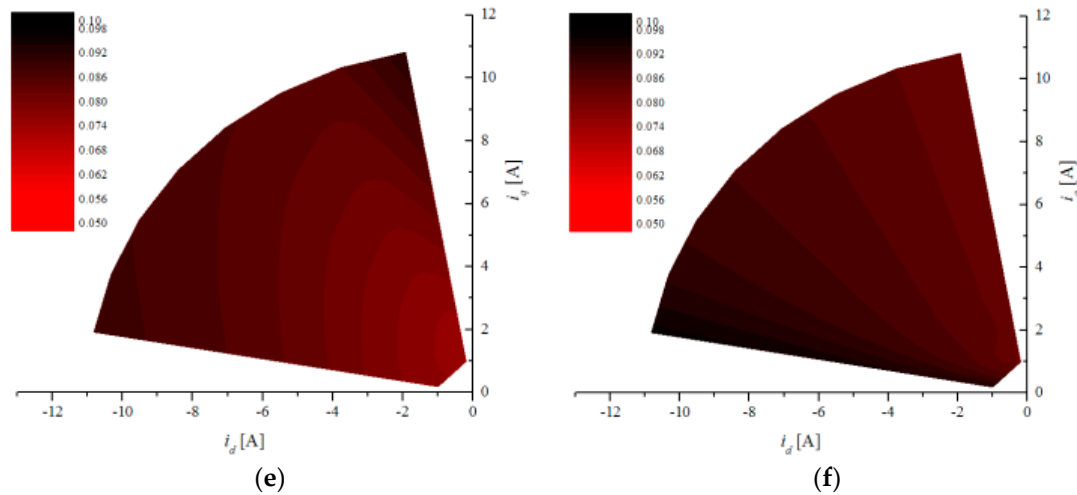


Figure 9. *d*- and *q*-axis inductance maps: (a) L_d at $-40\text{ }^\circ\text{C}$; (b) L_q at $-40\text{ }^\circ\text{C}$; (c) L_d at $20\text{ }^\circ\text{C}$; (d) L_q at $20\text{ }^\circ\text{C}$; (e) L_d at $80\text{ }^\circ\text{C}$; (f) L_q at $80\text{ }^\circ\text{C}$.

The basic parameters of the SPMSM are listed in Table 1. The motor parameters with nonlinear characteristics, as shown in Figures 8 and 9, were applied using a look-up table. The proposed estimation method of motor parameter R_s was modeled and simulated in MATLAB Simulink. The motor model for the simulation is shown in Figure 10. The stator resistance was determined by the stator resistance table according to the stator winding temperature. The inductances were determined by the inductance a three-dimensional table according to current and rotor temperature.

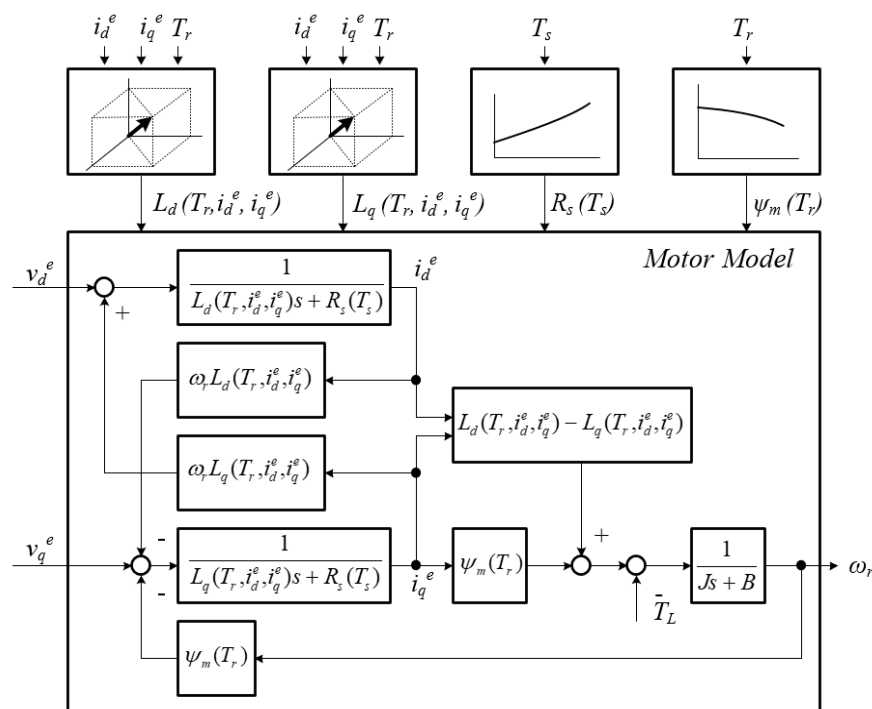


Figure 10. Motor simulation model.

The SPMSM controller and the motor model were configured as shown in Figure 11, based on the speed controller. To verify the proposed method, the simulation for the temperature estimation method was performed at 1000 rpm and 0.2 Nm. The rotor and the stator temperatures were assumed to be $20\text{ }^\circ\text{C}$ and $60\text{ }^\circ\text{C}$, respectively.

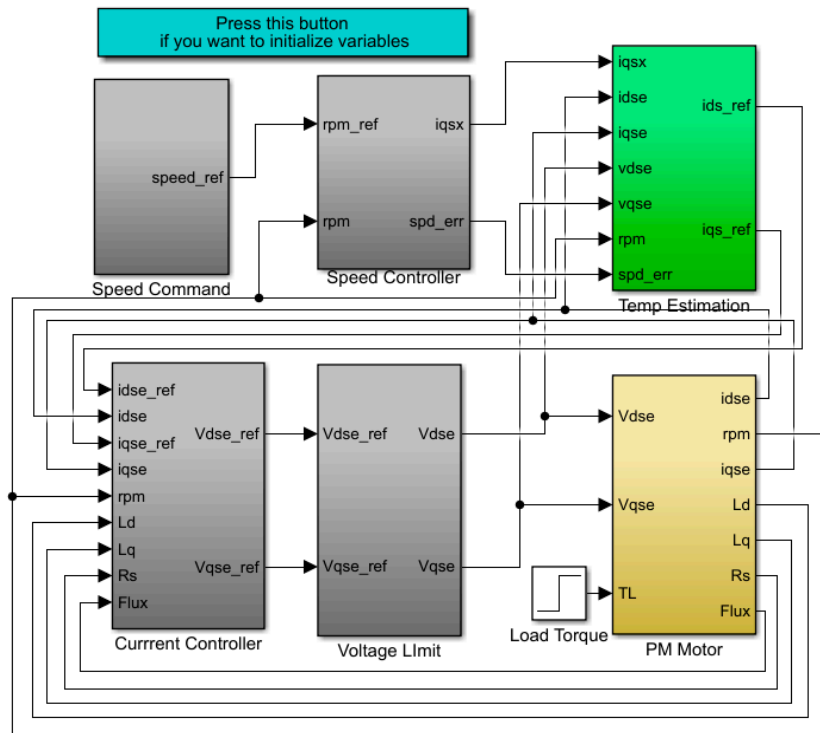
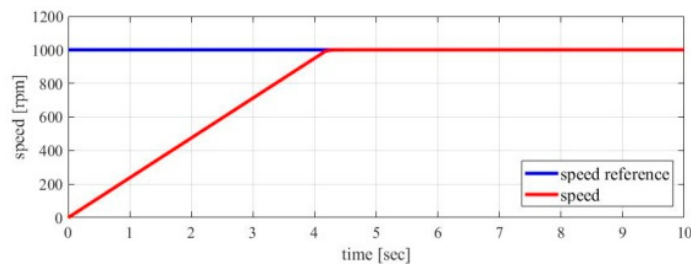
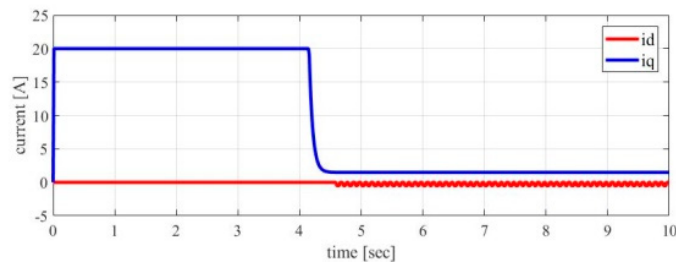


Figure 11. Simulation model for stator winding estimation.

Figure 12 shows the simulation results for the stator winding temperature estimation. In the steady-state, where the target speed is reached, the motor parameter estimation method, through the d -axis current injection, is operating. The stator winding temperature was estimated through the motor parameter estimation. As shown in Figure 12, the stator winding temperature was estimated almost exactly.



(a)



(b)

Figure 12. Cont.

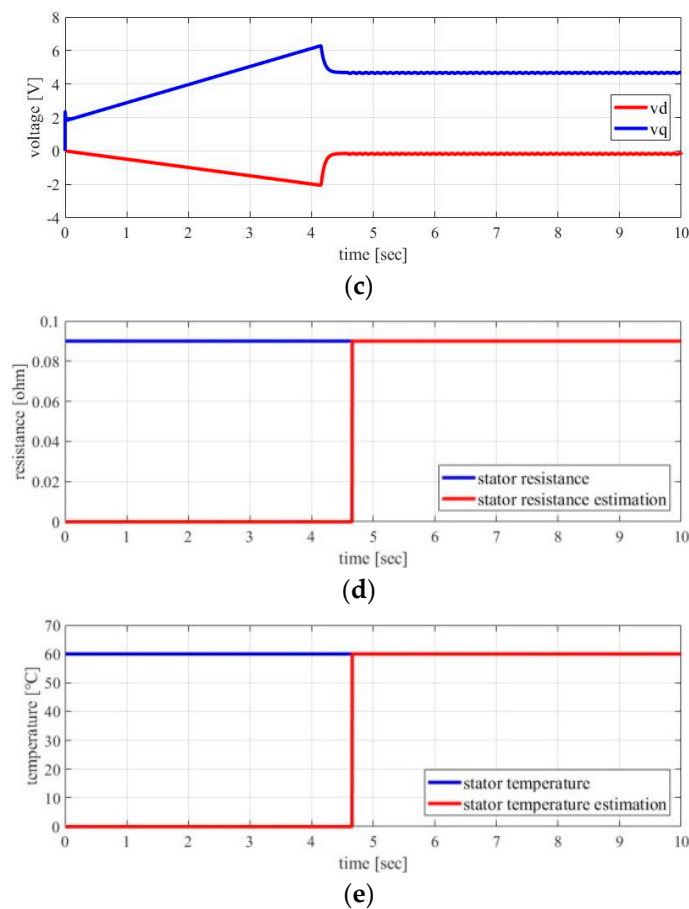


Figure 12. Simulation results: (a) motor speed; (b) i_d and i_q ; (c) v_d and v_q ; (d) stator resistance estimation; (e) stator winding temperature.

5. Experimental Results

Figure 13 shows an experimental setup for validating the stator winding temperature estimation method, consisting of a prototype SPMSM and an inverter. The test motor is the outer-rotor-type for a drone, and the specifications are shown in Table 1. A 20 kHz PWM frequency was applied to the inverter, and the stator winding estimator was operated synchronously with the PWM frequency. For comparison with the estimation value, the negative temperature coefficient (NTC) thermistor 103NT-4-R025H34G temperature sensor was attached inside the stator winding. A characteristic of the NTC thermistor is that the resistance decreases when the temperature increases. The stator winding temperature was obtained from the NTC thermistor, and the accuracy of the estimated stator winding temperature was evaluated. For the competitive experiment, the test was carried out with the actual load fan. The stator winding temperature estimation was compared until temperature saturation at 1000 rpm, where the drone fan motor was mainly operated.

Figure 14 shows the phase current, q -axis current, and d -axis current waveforms for when the d -axis current was or was not injected at 1000 rpm. For estimating the stator winding temperature, a d -axis current of -1 A was injected. The magnitude of the phase current was slightly increased due to the d -axis current injection.

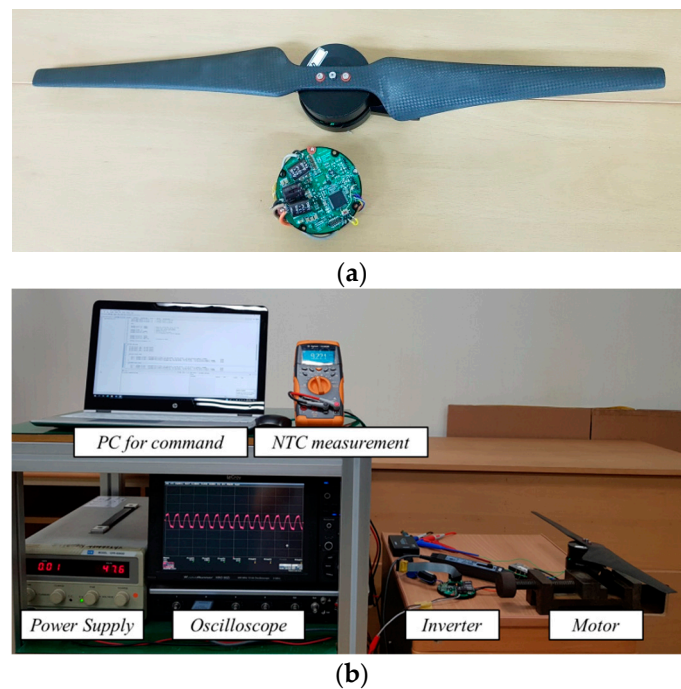


Figure 13. (a) Test motor/inverter; (b) experimental setup.

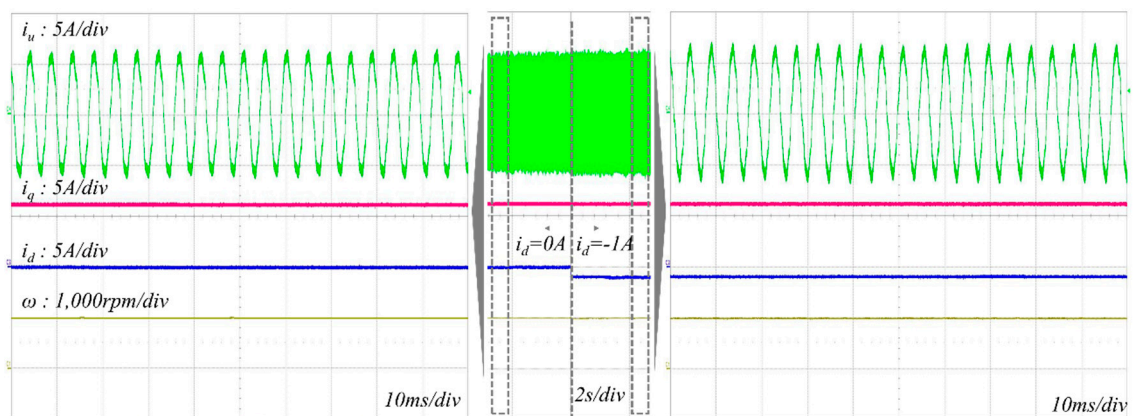


Figure 14. Phase current waveforms when d -axis current was injected at 1000 rpm.

Figure 15 shows the stator winding temperature estimation results for no load and fluid load. At no load, stator temperature saturation occurred after approximately 8 min of motor operation, and the temperature increased to 32 °C. However, the stator temperature saturation occurred after approximately 2 min of motor operation at the fluid load, and the temperature increased to 30 °C. In the fluid load, the fan affects the temperature of the motor, and the stator temperature saturated at lower temperatures than at no load. The maximum error of temperature estimation was measured at approximately 2 °C. The stator winding temperature estimation was verified for both no load and fluid load.

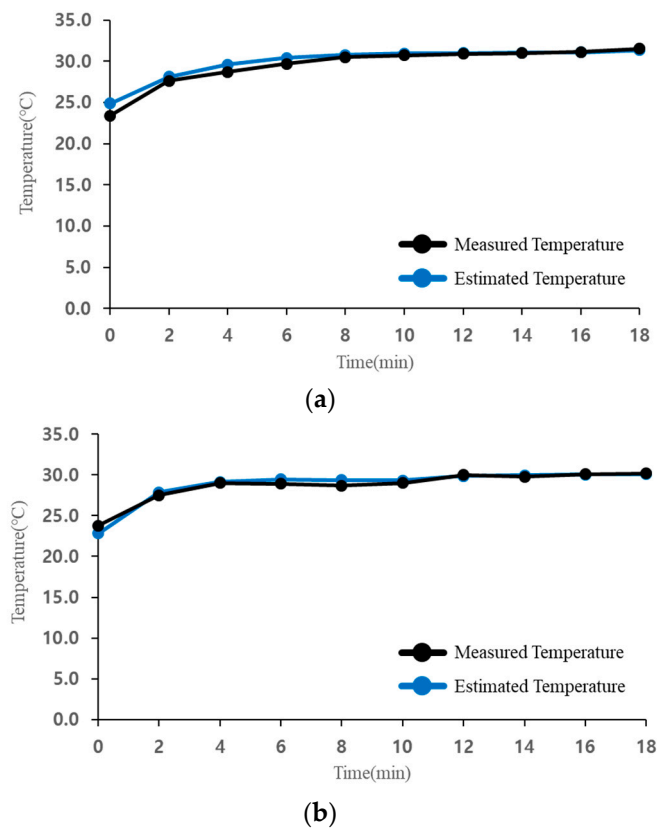


Figure 15. Stator winding temperature estimation results at (a) no load; (b) fluid load.

6. Conclusions

We presented a stator winding temperature estimation method for SPMSMs without additional temperature sensors. To estimate the stator winding temperature, the stator resistance was estimated using the proposed d -axis current injection. To evaluate the possibilities for the proposed estimation method, simulations and experimental tests were performed. The test and simulation results showed similar trends. According to both the simulation and the test results, the proposed estimation method demonstrated potential for winding temperature estimation without additional temperature sensors. However, after estimating the stator winding temperature, a control strategy is needed to limit stator winding temperature in the SPMSM control system. Future work will focus on developing such a control strategy to limit stator winding temperature.

Author Contributions: B.-S.J. implemented mathematical modeling and performed the experimental test; J.S.P. designed and performed the control simulation; J.-H.C. analyzed the simulation and experimental results. K.-D.L. performed the simulation and analyzed the validated result data through FEM; C.-Y.W. guided and revised the manuscript. All authors discussed the results and contributed to writing the paper.

Funding: This research was funded by the Ministry of Trade, Industry & Energy (MOTIE, Korea) under Industrial Technology Innovation Program Grant 10063006, and by the Korea Institute of Energy Technology Evaluation and Planning (KETEP) and the the Ministry of Trade, Industry & Energy (MOTIE) of the Republic of Korea under Grant 20172010105270.

Conflicts of Interest: The authors declare no conflicts of interest.

References

1. Reigosa, D.; Fernandez, D.; Tanimoto, T.; Kato, T. Comparative analysis of BEMF and pulsating high-frequency current injection methods for PM temperature estimation in PMSMs. *IEEE Trans. Power Electron.* **2017**, *32*, 3691–3699. [[CrossRef](#)]
2. Zhang, P.; Lu, B.; Habetler, T.G. A remote and sensorless stator winding resistance estimation method for thermal protection of soft-starter-connected induction machines. *IEEE Trans. Ind. Electron.* **2008**, *55*, 3611–3618. [[CrossRef](#)]
3. He, L.; Cheng, S.; Du, Y.; Harley, R.G.; Habetler, T.G. Stator temperature estimation of direct-torque-controlled induction machines via active flux or torque injection. *IEEE Trans. Power Electron.* **2015**, *30*, 888–899. [[CrossRef](#)]
4. Choi, J.-H.; Gu, B.-G.; Won, C.-Y. Modeling and analysis of PMSMs under inter turn short faults. *J. Electr. Eng. Technol.* **2013**, *8*, 1243–1250. [[CrossRef](#)]
5. Gu, B.-G. Study of IPMSM interturn faults part I: Development and analysis of models with series and parallel winding connections. *IEEE Trans. Power Electron.* **2016**, *31*, 5931–5943. [[CrossRef](#)]
6. Gu, B.-G. Study of IPMSM interturn faults part II: Online fault parameter estimation. *IEEE Trans. Power Electron.* **2016**, *31*, 7214–7223. [[CrossRef](#)]
7. Mellor, P.H.; Roberts, D.; Turner, D.R. Lumped parameter thermal model for electrical machines of TEFC design. *IEE Proc. B Electr. Power Appl.* **1991**, *138*, 205–218. [[CrossRef](#)]
8. Bousbaine, A.; McCormick, M.; Low, W.F. In-situ determination of thermal coefficients for electrical machines. *IEEE Trans. Energy Convers.* **1995**, *10*, 385–391. [[CrossRef](#)]
9. Moreno, J.F.; Hidalgo, F.P.; Martinez, M.D. Realisation of tests to determine the parameters of the thermal model of an induction machine. *IEE Proc. Electr. Power Appl.* **2001**, *148*, 393–397. [[CrossRef](#)]
10. Boglietti, A.; Cavagnino, A.; Lazzari, M.; Pastorelli, M. A simplified thermal model for variable speed self cooled industrial induction motor. *IEEE Trans. Ind. Appl.* **2003**, *39*, 945–952. [[CrossRef](#)]
11. Cheng, S.; Du, Y.; Restrepo, J.A.; Zhang, P.; Habetler, T.G. A nonintrusive thermal monitoring method for closed-loop drive-fed induction machines. In Proceedings of the 2011 IEEE Energy Conversion Congress and Exposition, Phoenix, AZ, USA, 17–22 September 2011.
12. Cheng, S.; Du, Y.; Restrepo, J.A.; Zhang, P.; Habetler, T.G. A nonintrusive thermal monitoring method for induction motors fed by closed-loop inverter drives. *IEEE Trans. Power Electron.* **2012**, *27*, 4122–4131. [[CrossRef](#)]
13. Lee, S.B.; Habetler, T.G.; Harley, R.G.; Gritter, D.J. A stator and rotor resistance estimation technique for conductor temperature monitoring. In Proceedings of the Thirty-Fifth IAS Annual Meeting and World Conference on Industrial Applications of Electrical Energy, Italy, Rome, 8–12 October 2000.
14. Uddin, M.N.; Radwan, T.S.; Rahman, M.A. Performance of interior permanent magnet motor drive over wide speed range. *IEEE Trans. Energy Convers.* **2002**, *17*, 79–84. [[CrossRef](#)]
15. Nam, K. *AC Motor Control and Electric Vehicle Applications*; CRC Press: Boca Raton, FL, USA, 2010; ISBN 978-1-4398-1963-0.
16. Park, J.S.; Nam, K. Dual inverter strategy for high speed operation of HEV permanent magnet synchronous motor. In Proceedings of the 2006 IEEE Industry Applications Conference Forty-First IAS Annual Meeting, Tampa, FL, USA, 8–12 October 2006.
17. Sun, H.; Jing, K.; Dong, Y.; Zheng, Y. Current dynamically predicting control of PMSM targeting the current vectors. *J. Electr. Eng. Technol.* **2015**, *10*, 1058–1065. [[CrossRef](#)]
18. Atallah, K.; Howe, D.; Stone, D. Rotor loss in permanent-magnet brushless AC machines. *IEEE Trans. Ind. Appl.* **2000**, *36*, 1612–1618. [[CrossRef](#)]
19. Reigosa, D.D.; Briz, F.; Degner, M.W.; Garcia, P.; Guerrero, J.M. Magnet temperature estimation in surface PM machines during six-step operation. *IEEE Trans. Ind. Appl.* **2012**, *48*, 2353–2361. [[CrossRef](#)]

